Biosorption of Rhodamine 6G from aqueous solutions onto almond shell (*Prunus dulcis*) as a low cost biosorbent

Hasan Basri Senturk [1], Duygu Ozdes [1], Celal Duran *

Department of Chemistry, Karadeniz Technical University, Faculty of Arts and Sciences, 61080 Trabzon, Turkey

ABSTRACT

This work presents an alternative methodology for removal of a dyestuff, Rhodamine 6G (R6G), from aqueous solutions by using a new biosorbent, almond shell (*Prunus dulcis*), in a batch biosorption technique. The characterization of the biosorbent was performed by using FTIR and SEM techniques. The biosorption characteristics of R6G onto almond shell (AS) was investigated with respect to the changes in initial pH of dye solutions, contact time, initial R6G concentration, AS concentration, temperature etc. The influences of ionic strength on the biosorption process were also investigated. The biosorption kinetics was followed by pseudo-second-order model for all investigated initial R6G concentrations. Experimental data showed a good fit with both the Langmuir and Freundlich isotherm models. The monolayer biosorption capacity of AS was found to be 32.6 mg g^{-1} by using Langmuir model equations. Thermodynamic parameters including the Gibbs free energy (ΔG^o), enthalpy (ΔH^o), and entropy (ΔS^o) changes indicated that the biosorption of R6G onto AS was feasible, spontaneous and endothermic in the temperature range of 0–40 °C.

Crown Copyright © 2009 Published by Elsevier B.V. All rights reserved.

1. Introduction

Most of the industries including textiles, pulp mills, leathers, plastics, cosmetics, foods and pharmaceuticals require the use of various raw materials and chemicals so the resulting wastewaters contain many harmful elements and compounds such as organic materials and heavy metals. Among the different organic compounds released along with industrial effluents, dyes and pigments are one of the most dangerous and considerable water pollutants since some dyes cause toxic or mutagenic, teratogenic and carcinogenic effects on aquatic life and also on humans when present in waters even at low concentrations [1,2]. The presence of dyes in natural streams reduces light penetration, retards photosynthetic activity, inhibits the growth of biota, and also has a tendency to chelate metal ions that produce micro-toxicity to fish and other organisms [3]. In addition, as a result of direct contact, inhalation or ingestion of dyes can cause eye burns, rapid or difficult breathing, nausea and vomiting, etc. on humans [4]. There are many structural varieties of dyes, such as acidic, basic, disperse, azo, diazo, anthroquinone based and metal complex dyes.

The dye R6G, used in present study, is a basic dye and used widely in acrylic, nylon, silk, and wool dyeing [5]. Because of the common utilization of R6G in industrial applications, the removal of it from industrial wastewaters is important in terms of protection of public health, environment and aquatic life.

The methods employed for removal of dyes from contaminated wastewaters include coagulation, flocculation, biological oxidation, solvent extraction, chemical precipitation, reverse osmosis, ion exchange, filtration, and membrane processes, etc. [6]. Most of these techniques have significant disadvantages including incomplete dye removal, high reagent and energy necessity, low selectivity, high capital and operational cost and generation of secondary wastes that are difficult to be disposal. On the other hand, the development of biosorption technique represents a powerful alternative for the removal of dyes and also other pollutants like heavy metals from industrial wastewaters. Biosorption is the process by which a solid living or non-living biosorbent can attract a component to its surface in aqueous solution and form an attachment via a physical or chemical bond, thus removing the component from the liquid phase. The major advantages of biosorption over conventional treatment methods include; low cost, high efficiency, minimization of chemical or biological sludge, no additional nutrient requirement, regeneration of biosorbent and possibility of sorbate recovery [7,8]. The agricultural and forestry products have a great potential to be used as biosorbents. Some of the reported low cost biosorbents include palm ash [9], de-oiled soya [10], broad bean peels [11], durian peel [12], rice husk [13], Nordmann fir leaves [14] and neem sawdust [15], etc. These types of biosorbents contain polysaccharides and proteins having various functional groups such as carboxyl, hydroxyl and phosphates [16]. The biosorption of dye molecules by these materials might be associated with these functional groups.

* Corresponding author. Tel.: +90 462 3774241; fax: +90 462 3253196.
 E-mail addresses: senturk@ktu.edu.tr (H.B. Senturk), duyguozdes@hotmail.com
(D. Ozdes), cduran@ktu.edu.tr (C. Duran).
 [1] Tel.: +90 462 3772498; fax: +90 462 3253196.

The AS is one of the most abundant, effective and cheap material. Hence, the AS was selected as a biosorbent for removal of R6G from aqueous solutions, in this study. 'AS' is the name of ligneous material forming the thick endocarp or husk of the almond tree, scientifically known as *Prunus dulcis*. When the fruit is processed to obtain the edible seeds, big ligneous fragments are separated. These materials remain available as a waste product for which no important industrial use has been developed [17].

The aim of present study was to evaluate the applicability of a new biosorbent, AS (*P. dulcis*), in removal of R6G from aqueous solutions by biosorption process. The different parameters such as initial solution pH, contact time, initial R6G and AS concentration, temperature and ionic strength were evaluated. The isotherm and kinetics as well as thermodynamic parameters for the adsorption of R6G dye onto the AS were calculated.

2. Materials and methods

2.1. Sorbate: R6G

The dye R6G, used in present study, is a cationic dye. Its Colour Index is (CI) 45,160, chemical formula is $C_{28}H_{31}ClN_2O_3$, formula weight (FW) is 479.02 g mol^{-1}, and absorbance maximum (λ_{max}) is 547 nm.

2.2. Preparation of biosorbent

The AS, (*P. dulcis*) which was used as a biosorbent in this study, collected from a local market in Turkey. Before use, it was washed with deionized water for several times to remove surface impurities then dried for 4 days at 40 °C. The dried AS samples were ground in a blender and sieved to obtain a particle size of <150 μm and stored in glass containers to use for biosorption experiments.

2.3. Biosorption experiments

All chemicals were of analytical reagent grade and were purchased from Merck (Darmstadt, Germany). All glassware and sample bottles were cleaned by soaking overnight in 10% (w/v) HNO_3 and the rinsing with deionized water for several times. A stock solution of R6G was prepared as 5000 mg L^{-1} in deionized water. The required concentration of R6G solutions were prepared by appropriate dilutions of the stock solutions. The initial pH of the solutions was adjusted to 8.0 by using either 0.1 M HCl or 0.1 M NaOH solutions. The biosorption tests of R6G onto AS were studied by using a batch process by mixing 100 mg of AS (10 g L^{-1}) with 10 mL of R6G solutions in the concentration range of 100–1000 mg L^{-1} in a polyethylene centrifuge tube. The mixtures were agitated at a speed of 400 rpm on a mechanical shaker (Edmund Bühler GmbH) for 2 h to reach equilibrium. After equilibrium, the biosorbent was separated from the dye solution by filtration using 0.45 μm nitrocellulose membrane (Sartorius Stedim Biotech. GmbH) and the remaining concentrations of R6G in the filtrate were determined by using a double beam UV–Vis spectrophotometer (Unicam UV-2) at wavelength of 547 nm. All of the experiments were triplicated to check the reproducibility of data and the averages of the results were used for data analysis. The concentration retained in the biosorbent phase (q_e, mg g^{-1}) was calculated by using the following equation;

$$q_e = \frac{(C_o - C_e)V}{m_s} \tag{1}$$

C_o (mg L^{-1}) is the initial concentration of R6G solution, C_e (mg L^{-1}) is the equilibrium concentration of R6G in aqueous solution, V (L) is the volume of solution, m_s (g) is the mass of the biosorbent and q_e (mg g^{-1}) is the calculated R6G biosorption amount onto AS.

3. Results and discussion

3.1. Fourier Transform Infrared (FTIR) Spectroscopy and Scanning Electron Microscopy (SEM) studies

The IR spectra of the AS and R6G loaded AS were obtained to determine the surface functional groups by using Perkin Elmer 1600 FTIR spectrophotometer. The positions of the peaks obtained from FTIR spectra of AS and R6G loaded AS were approximately similar but the band intensities decreased from 56 to 52% in the FTIR spectrum of R6G loaded AS, as expected (figure not shown). The FTIR measurements show the presence of following groups: O–H (3400 cm^{-1}; stretch vibration), C–H aromatic and aliphatic (2930 cm^{-1}; stretch vibration), C=O (1740 cm^{-1}; stretch vibration), C=C aromatic (1608 and 1505 cm^{-1}; stretch vibration), C–H (1465 and 1378 cm^{-1}; deformation vibration) and C–O (1040 cm^{-1}; stretch vibration). Similar results were obtained by Estevinho et al. [18] with pentachlorophenol adsorption by AS residues.

SEM analyses were applied on the AS and also R6G loaded AS by a JSM 6400 Scanning Microscope apparatus in order to disclose the surface texture and morphology of the biosorbent. The SEM micrographs of AS and R6G loaded AS are shown in Fig. 1a and b. The AS has considerable numbers of heterogeneous pores where there is a good possibility for R6G trapped and biosorbed. The structure of AS changed upon R6G biosorption and exhibited a tendency to form agglomerates.
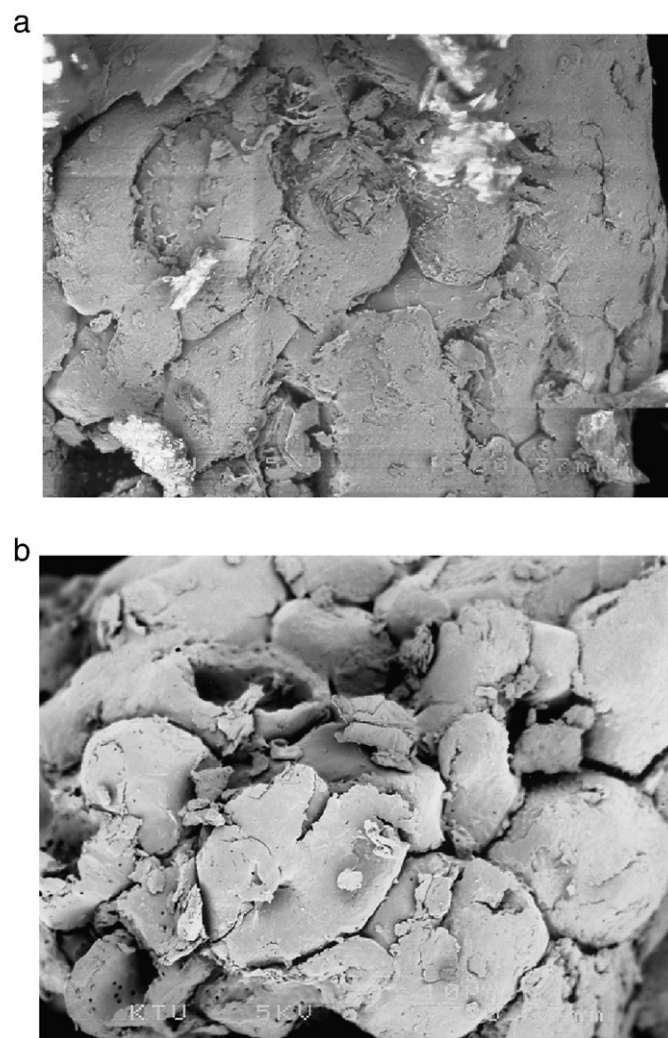

Fig. 1. SEM of (a) AS and (b) R6G loaded AS (magnification: 500×).

3.2. Effect of initial pH

The pH of the dye solution is one of the most important variables because the protonation of the functional groups on the biosorbent surface, and the chemistry of dye molecules are strongly affected by the pH of the solution. The effect of initial solution pH on the biosorption of R6G was evaluated over a range of pH values from 3 to 9 by using initial R6G concentration of 100 mg L^{-1} and AS concentration of 10 g L^{-1} (Fig. 2).

The amount of dye uptake increased from 4.3 mg g^{-1} (43% removal) to 8.8 mg g^{-1} (88% removal) for an increase at pH value from 3 to 9. At lower pH values, the number of negatively charged biosorbent sites decreased so the surface of the biosorbent was associated with hydronium ions. As the pH of the dye solution decreased, the electrostatic repulsion between positively charged dye cations and AS surface sites and also competing effects of hydronium ions with dye cations increased so the uptake of R6G decreased. On the other hand, in alkaline medium, the biosorbent surface sites were more negatively charged so the electrostatic interaction of R6G with negatively charged biosorbent surface increased which favored the removal of dye cations [19]. As a result, initial pH was selected as 8.0 for further biosorption experiments.

3.3. Effect of contact time and initial R6G concentration

The effects of initial concentration of R6G on the rate of dye biosorption onto AS were studied at a constant AS concentration (10 g L^{-1}) and at different initial R6G concentration (100, 400, 600 and 1000 mg L^{-1}) at initial pH 8.0 for different time intervals from 1 to 480 min at room temperature (Fig. 3). The R6G uptake was rapid for the first 30 min for all investigated initial dye concentrations, and thereafter it continued at a slower rate and finally reached to the saturation. This may be explained by the fact that the biosorption sites were open at the beginning of the biosorption so R6G interacted easily with these sites. The equilibrium was attained within the contact time of 60 min for the initial dye concentrations of 100, 400 and 600 mg L^{-1} and the contact time of 120 min for the initial dye concentration of 1000 mg L^{-1}. After these periods of time, the concentration of R6G in liquid phase remained almost constant. In order to make sure whether the sufficient contact time was obtained, further biosorption experiments were carried out for 120 min.

At equilibrium, the amount of R6G uptake increased from 8.8 to 23.5 mg g^{-1} whereas biosorption percentage decreased from 73 to 22.4% with increasing the initial R6G concentration from 100 to 1000 mg L^{-1}. This can be explained by the fact that the initial R6G
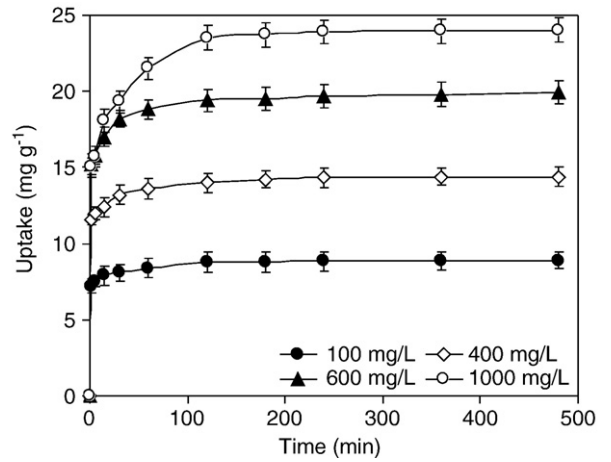

Fig. 3. Effect of contact time and initial R6G concentration.

concentration acts as a driving force to overcome mass transfer resistance for R6G transport between the solution and the surface of the AS. At lower concentrations almost all the dye molecules were biosorbed quickly on the surface, but increasing in initial R6G concentrations led to fast saturation of AS surface so most of the dye molecules diffuse slowly inside the pores [5].

3.4. Effect of AS concentration

The effects of AS concentration on the uptake of R6G from aqueous solutions were studied by using initial R6G concentration of 410 mg L^{-1} at initial pH 8.0 and varying AS concentration from 1.0 to 20.0 g L^{-1}. As the AS concentrations were increased from 1 to 20 g L^{-1}, the equilibrium biosorption capacity of AS, q_e, decreased from 30 to 9.5 mg g^{-1}, whereas, the R6G removal efficiency increased from 14.3 to 90.5% (Fig 4). The increase in biosorption percentage of R6G was probably due to the increased more availability of active biosorption sites with the increase in AS concentration. However the decrease in equilibrium biosorption capacity can be explained with the reduction in the effective surface area. In other words, the biosorbent surface sites remain unsaturated during the biosorption process [20].
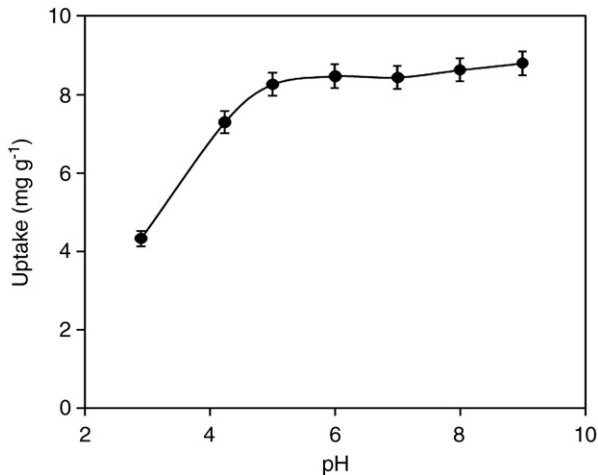

Fig. 2. Effect of pH on R6G uptake by AS (initial R6G conc.: 100 mg L^{-1}, AS conc.: 10 g L^{-1}, contact time: 2 h).
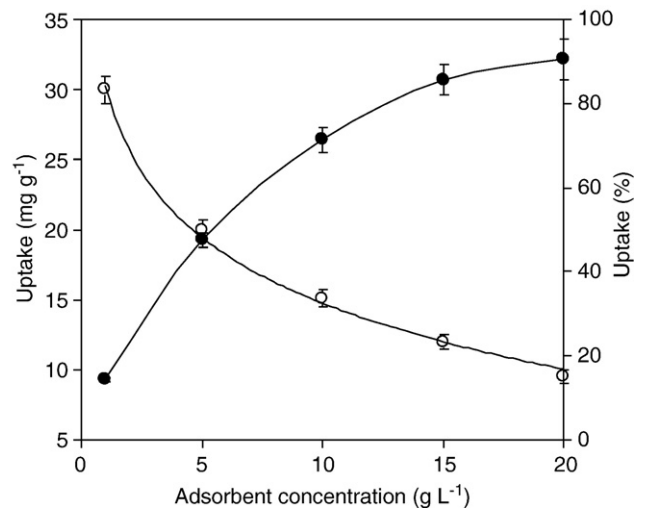

Fig. 4. Effect of AS concentration on R6G uptake (pH: 8.0, initial R6G conc.: 410 mg L^{-1}, contact time: 2 h).

3.5. Effect of temperature

Temperature has significant effects on the biosorption efficiency depending on the structure and surface functional groups of a sorbent. Hence the effect of temperature on the biosorption of R6G onto AS was investigated in the temperature range of 0–40 °C by using initial R6G concentration of 100 mg L^{-1} at initial pH 8.0 and AS concentration of 10 g L^{-1}. The temperature of R6G solutions was controlled by a cryostat (Nüve BD 402, temperature range from −10 to +40 °C). The biosorption of R6G onto AS increased from 6.0 mg g^{-1} (60% removal) to 8.5 mg g^{-1} (85% removal) when the temperature increased from 0 to 40 °C, indicating that the biosorption process was endothermic in nature. The increase in the biosorption capacity of AS with temperature may be results of increase in the mobility of dye cations and also increase in number of available active surface sites on the AS for biosorption.

3.6. Effect of ionic strength

The removal efficiency of dyes may be changed with different concentrations of electrolytes present in the dye medium, hence the effects of ionic strength on the uptake of R6G from aqueous solutions should be studied. For this, biosorption studies were carried out by adding various concentrations (in the range of 0.01–0.2 M) of KCl, Na$_2$SO$_4$ and NaNO$_3$ solutions individually, in 105 mg L^{-1} of R6G solutions containing 10 g L^{-1} of AS, and the present biosorption process was applied to these solutions. The amount of R6G removal was influenced by the presence of electrolytes. In the absence of salts the amount of R6G uptake was 8.8 mg g^{-1} (84% removal). It was observed that, at lower concentrations of Na$_2$SO$_4$ and NaNO$_3$ solutions (in the range of 0.01–0.1 M), the R6G uptake was found to gradually increase, which can be explained by the salting out effect [21] whereas as the concentrations of Na$_2$SO$_4$ and NaNO$_3$ were increased from 0.1 to 0.2 M, the amount of R6G uptake decreased from 8.9 and 8.7 mg g^{-1}, to 8.5 and 8.3 mg g^{-1}, and percentage removal efficiency decreased from 85.0 and 83.2% to 81.0 and 79.0%, respectively. As the concentration of KCl was increased from 0 to 0.2 M, the amount of R6G uptake decreased from 8.8 mg g^{-1} (84.0% removal) to 5.0 mg g^{-1} (48% removal) (Fig. 5). The interfere effects of KCl salt was much more apparent than those of Na$_2$SO$_4$ and NaNO$_3$ salts. These results can be attributed by the fact that the active sites of the biosorbent may be blocked in the presence of KCl salt and higher concentrations of Na$_2$SO$_4$ and NaNO$_3$ salts so R6G molecules are hindered to bind the surface of the biosorbent.
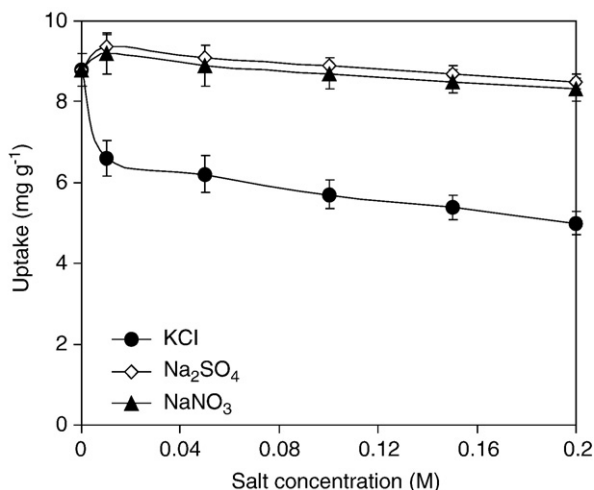

Fig. 5. Effect of ionic strength on the R6G uptake (pH: 8.0, initial R6G conc.: 105 mg L^{-1} AS conc.: 10 g L^{-1}, contact time: 2 h).

3.7. Biosorption isotherms

Sorption isotherms define the equilibrium relationship between sorbent and sorbate. In other words, how the sorbed molecules interact with sorbents when the sorption process approaches to an equilibrium state can be described by sorption isotherms [22]. Sorption isotherms also ensure many fundamental physicochemical data to estimate the applicability of sorption processes. Sorption isotherms are characterized by certain constants which values express the surface properties and affinity of the sorbent and can also used to find the sorptive capacity of a mass [23]. Different isotherm models are available, and two of them are selected in this study: Langmuir and Freundlich models, due to their simplicity and reliability.

3.7.1. Langmuir isotherm model

The Langmuir isotherm model predicts the existence of monolayer coverage of the sorbate molecules over a homogeneous sorbent surface, and there is no important interaction among the sorbed species. The Langmuir model also assumes that the sorbent surface contains only one type of binding site so the energy of sorption is constant. The Langmuir isotherm model has the following form [24];

$$q_e = \frac{b q_{max} C_e}{1 + b C_e} \qquad (2)$$

where q_e (mg g^{-1}) is the amount of the dye sorbed per unit mass of sorbent, C_e (mg L^{-1}) is the equilibrium dye concentration in the solution, q_{max} (mg g^{-1}) is the Langmuir constant related the maximum monolayer sorption capacity and b (L mg^{-1}) is the constant related to the free energy or net enthalpy of adsorption. The Langmuir model in linear form;

$$\frac{C_e}{q_e} = \frac{C_e}{q_{max}} + \frac{1}{b q_{max}} \qquad (3)$$

The linear plot of C_e/q_e versus C_e shows that sorption obeys the Langmuir model and the constants q_{max} and b are evaluated from slope and intercept of the linear plot, respectively.

The essential characteristics of Langmuir isotherm can be described by means of 'R_L' a dimensionless constant referred to as separation factor or equilibrium parameter. R_L can be calculated using the following equations [25];

$$R_L = \frac{1}{1 + b.C_o} \qquad (4)$$

where C_o (mg L^{-1}) is the initial concentration of sorbate and b (L mg^{-1}) is the Langmuir constant described above.

The R_L parameter is considered as more reliable indicator of sorption. There are four probabilities for the R_L value:

- for favorable sorption $0 < R_L < 1$,
- for unfavorable sorption $R_L > 1$,
- for linear sorption $R_L = 1$,
- for irreversible sorption $R_L = 0$.

The experimental equilibrium data of R6G were compared with the theoretical equilibrium data obtained from Langmuir isotherm model (Fig 6). The adsorption data were analyzed according to the linear form of Langmuir isotherm (Eq. (3)). The values of q_{max} and b obtained from the slope and intercept of the linear plot of C_e/q_e versus C_e (figure not shown) were found to be 32.6 mg g^{-1} and 0.0035 L mg^{-1} respectively, with correlation coefficient (R^2) of 0.981. The R_L values ranged from 0.214 to 0.700 between 100 and 1000 mg L^{-1} of initial R6G concentration and approached zero with increase in the C_o value, indicated that the AS is a suitable biosorbent for the biosorption of R6G from aqueous solutions. From the results, the biosorption pattern of R6G onto AS was
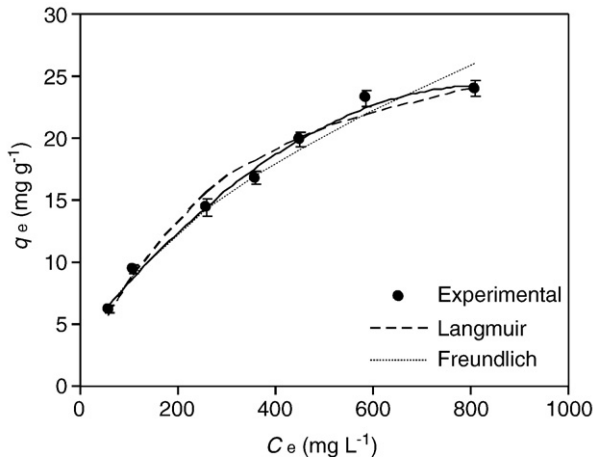
Fig. 6. Equilibrium isotherms of R6G onto AS.

well fitted with the Langmuir isotherm model. This may be due to homogeneous distribution of active sites on the surface of the AS.

3.7.2. Freundlich isotherm model

The Freundlich isotherm model assumes a heterogeneous sorption surface with sites that have different energies of sorption and provides no information on the monolayer adsorption capacity [26]. The Freundlich model has the form;

$$q_e = K_f C_e^{1/n} \qquad (5)$$

where K_f is a constant related to sorption capacity (mg g^{-1}) and $1/n$ is an empirical parameter related to sorption intensity. The value of n varies with the heterogeneity of sorbent and gives an idea for the favorability of sorption process. The value of n should be less than 10 and higher than unity for favorable sorption conditions.

The Freundlich model in linear form;

$$\ln q_e = \ln K_f + \frac{1}{n} \ln C_e \qquad (6)$$

The experimental equilibrium data of R6G were also compared with the theoretical equilibrium data obtained from Freundlich isotherm model (Fig. 6). The values of Freundlich constants, K_f and $1/n$, were obtained according to the linear form of the Freundlich isotherm (Eq. (6)) and found to be 0.740 mg g^{-1} and 0.532 respectively, with correlation coefficient (R^2) of 0.989. The Freundlich constant $1/n$ was smaller than unity indicated that the biosorption process was favorable under studied conditions. It is clear that the biosorption pattern of R6G onto AS was well fitted with both the Langmuir and Freundlich isotherm models. This may be due to both homogeneous and heterogeneous distribution of active sites on the surface of the AS.

3.8. Biosorption kinetics

In order to predict the mechanism of the present biosorption process and evaluate the performance of the biosorbent for dye removal, three well-known kinetic models were used to fit the experimental data; pseudo-first-order, pseudo-second-order and intraparticle diffusion models.

3.8.1. Pseudo-first-order model

The pseudo-first-order kinetic model was described by Lagergren [27];

$$\frac{d_q}{d_t} = k_1(q_e - q_t) \qquad (7)$$

where q_e (mg g^{-1}) and q_t (mg g^{-1}) are the amounts of the dye biosorbed on the biosorbate at equilibrium and at any time t, respectively; and k_1 (min^{-1}) is the rate constant of the first order model. After integration and applying boundary conditions $q_t = 0$ at $t = 0$ and $q_t = q_t$ at $t = t$ the integrated form of Eq. (7) becomes;

$$\ln(q_e - q_t) = \ln q_e - k_1 t \qquad (8)$$

A straight line of $\ln(q_e - q_t)$ versus t suggests the applicability of this kinetic model and q_e and k_1 can be determined from the intercept and slope of the plot, respectively.

It is important to notice that the experimental q_e must be known for the application of this model. Table 1 shows the pseudo-first-order constants, q_e and k_1, along with the corresponding correlation coefficients for investigated initial R6G concentrations. The calculated $q_{e\ cal}$ values were not in a good agreement with the experimental values of $q_{e\ exp}$ and the correlation coefficients were found in the range from 0.824 to 0.927, which were relatively low. There was a deviation from the straight line of $\ln(q_e - q_t)$ versus t (figure not shown) after the first 30 min for all investigated initial dye concentrations, indicating that the pseudo-first-order model was only applicable for the first 30 min of biosorption. These observations suggested that the pseudo-first-order model is not suitable for modeling the biosorption of R6G onto AS.

3.8.2. Pseudo-second-order model

The pseudo-second-order model based on the assumption that the rate-limiting step is chemical sorption or chemisorption involving valance forces through sharing or exchange of electrons between sorbent and sorbate as covalent forces [28,29]. The model has the following form [30];

$$\frac{d_q}{d_t} = k_2(q_e - q_t)^2 \qquad (9)$$

where k_2 (g mg^{-1} min^{-1}) is the rate constant of the second-order equation; q_e (mg g^{-1}) is the maximum biosorption capacity; q_t (mg g^{-1}) is the amount of biosorption at time t (min).

Table 1
Parameters of pseudo-first-order, pseudo-second-order and intraparticle diffusion model.

C_o (mg L^{-1})	$q_{e\ exp}$ (mg g^{-1})	Pseudo-first-order			Pseudo-second-order			Intraparticle diffusion model				
		$q_{e\ cal}$ (mg g^{-1})	k_1 (min^{-1})	R^2	$q_{e\ cal}$ (mg g^{-1})	k_2 (g mg^{-1} min^{-1})	R^2	$k_{id,1}$ (mg g^{-1} min$^{-1/2}$)	R^2	$k_{id,2}$ (mg g^{-1} min$^{-1/2}$)	R^2	C (mg g^{-1})
100	8.9	1.58	−0.013	0.824	8.91	0.066	0.999	0.177	0.972	0.011	0.958	5.72
400	14.4	3.44	−0.017	0.873	14.45	0.035	0.999	0.308	0.978	0.035	0.787	9.15
600	19.9	4.86	−0.017	0.869	19.92	0.024	0.999	0.566	0.970	0.046	0.958	12.28
1000	24	8.33	−0.016	0.927	24.15	0.011	0.999	0.992	0.989	0.044	0.854	12.41

After definite integration by applying the conditions $q_t = 0$ at $t = 0$ and $q_t = q_t$ at $t = t$ the Eq. (9) becomes the following;

$$\frac{t}{q_t} = \frac{1}{k_2 q_e^2} + \frac{t}{q_e} \tag{10}$$

If second-order kinetics is applicable, the plot of t/q_t against t gives a straight line and q_e and k_2 can be obtained from the slope and intercept of the plot, respectively. For investigated initial dye concentrations, k_2 and $q_{e\ cal}$ values along with the corresponding correlation coefficients are presented in Table 1. The correlation coefficients were nearly equal to unity and calculated $q_{e\ cal}$ values were much close to the experimental values of $q_{e\ exp}$. The results indicated that the pseudo-second-order biosorption mechanism is predominant for the biosorption of R6G onto AS, and it is considered that the rate of the dye biosorption process is controlled by the chemisorption process.

3.8.3. Intraparticle diffusion models

In order to predict the rate controlling step of the R6G biosorption, intraparticle diffusion model has been used. Generally any sorption process involves three main successive transport steps which are (i) film diffusion, (ii) intraparticle or pore diffusion and (iii) sorption onto interior sites. The last step is considered negligible since it occurs rapidly and hence sorption should be controlled by either film diffusion or pore diffusion depending on which step is slower [31] The intraparticle diffusion model equation is expressed as [32];

$$q_t = k_{id} t^{1/2} + c \tag{11}$$

where q_t (mg g^{-1}) is the amount of sorption at time t (min) and k_{id} (mg g^{-1} min$^{-1/2}$) is the rate constant of intraparticle diffusion model. Fig. 7 shows the intraparticle mass transfer curves at various R6G concentrations. It was observed that the R6G biosorption process tends to be followed by two distinct phases. The first phase is attributed to the diffusion of R6G through the solution to the external surface of AS and the second phase indicates the intraparticle diffusion of R6G into the pores of AS. The intraparticle rate constants $k_{id,1}$ (for the first phase), $k_{id,2}$ (for the second phase) and c parameters were obtained from the plot of q_t versus $t^{1/2}$ and the results are given in Table 1. The values $k_{id,1}$ are higher than $k_{id,2}$ so it can be concluded that the rate-limiting step in present biosorption process is intraparticle diffusion. However the lines did not pass through the origin (the plots have intercepts in the R6G concentrations range of 100–1000 mg L^{-1}) indicating that the intraparticle diffusion model is not the only rate-limiting mechanism. Therefore it can be concluded that R6G biosorption onto AS is a complex process and both intraparticle
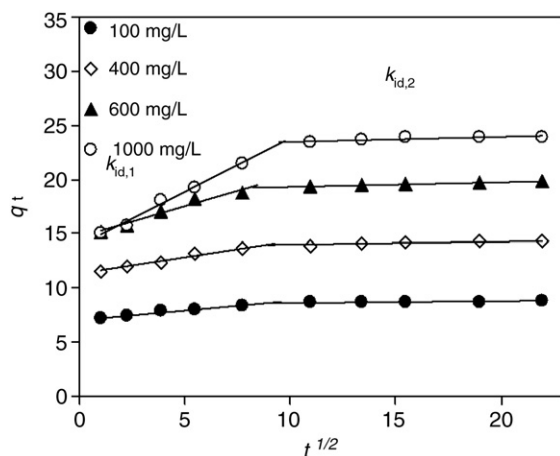
diffusion and surface sorption contributes to the rate-limiting step [33,34].

3.9. Thermodynamic studies

The thermodynamic parameters including Gibbs free energy change (ΔG^o), enthalpy (ΔH^o), and entropy change (ΔS^o), have a significant role to determine the feasibility, spontaneity and heat change for the biosorption process. These parameters can be calculated using the following equations [35];

$$\Delta G^o = -RT \ln K_d \tag{12}$$

where R is the universal gas constant (8.314 J mol^{-1} K^{-1}), T is the temperature (K), and K_d is the distribution coefficient. The K_d value was calculated using following equation [36];

$$K_d = q_e / C_e \tag{13}$$

where q_e and C_e are the equilibrium concentration of R6G on biosorbent (mg L^{-1}) and in the solution (mg L^{-1}), respectively. The enthalpy (ΔH^o), and entropy change (ΔS^o) of adsorption were estimated from the following equation;

$$\Delta G^o = \Delta H^o - T \Delta S^o \tag{14}$$

This equation can be written as;

$$\ln K_d = \frac{\Delta S^o}{R} - \frac{\Delta H^o}{RT} \tag{15}$$

The thermodynamic parameters of ΔH^o and ΔS^o were obtained from the slope and intercept of the plot between $\ln K_d$ versus $1/T$, respectively (figure not shown). The value of ΔG^o, ΔH^o, and ΔS^o for the biosorption of R6G onto AS at different temperatures is given in Table 2. The negative values of ΔG^o in the temperature range of 0–40 °C were due to the fact that the biosorption process was spontaneous and feasible thermodynamically. The negative value of ΔG^o has decreased from -0.92 to -4.45 kJ mol^{-1} with an increase in temperature from 0 to 40 °C, indicated that the spontaneous nature of biosorption of R6G was inversely proportional to the temperature. The positive value of ΔH^o (24.14 kJ mol^{-1}) suggested that the endothermic nature of biosorption while the positive value of ΔS^o (91.43 J mol^{-1} K^{-1}) indicated that the increasing randomness at the solid/solution interface during the biosorption of R6G onto AS. In addition, the magnitude of ΔH^o gives an idea about the type of sorption. Two main types of sorption may occur; physical and chemical. In physical sorption, the equilibrium is usually rapidly attained and easily reversible, because the energy requirements are small. The enthalpy for physical sorption is usually no more than 1 kcal mol^{-1} (4.2 kJ mol^{-1}) since the forces are weak. Chemical sorption involves forces much stronger than in physical adsorption, and the enthalpy for chemical sorption is more than 5 kcal mol^{-1} (21 kJ mol^{-1}) [37] so it seems that biosorption of R6G onto AS was almost a chemical process (Table 2).

Fig. 7. Intraparticle diffusion plots for adsorption of R6G onto AS.

Table 2
Thermodynamic parameters of the R6G biosorption onto AS at different temperatures.

T (°C)	ΔG^o (kJ mol^{-1})	ΔS^o (J mol^{-1} K^{-1})[a]	ΔH^o (kJ mol^{-1})[a]
0	−0.92		
10	−1.56		
20	−2.68	91.43	24.14
30	−3.65		
40	−4.45		

[a] Measured between 273 and 313 K.

4. Conclusions

The AS was found to be one of the most promising biosorbent for the uptake of dyes due to its low cost, easy availability, and high dye uptake capacity. The utilization of AS may be the main advantage of the present study because it is an agricultural waste material.

The R6G removal efficiency of the AS was tested in the light of equilibrium, kinetics and thermodynamics parameters. The kinetics of R6G biosorption onto AS followed by pseudo-second-order model. The biosorption pattern of R6G onto AS was well fitted with both the Langmuir and Freundlich isotherm models. The monolayer biosorption capacity of AS was found to be 32.6 mg g^{-1} by using Langmuir model equations. The thermodynamic parameters indicated that the biosorption of R6G onto AS was feasible, spontaneous and endothermic in nature.

The experimental results indicated that the AS (*P. dulcis*) can be successfully used for the removal of R6G from aqueous solutions.

Acknowledgments

References

[1] L. Laasri, M.K. Elamrani, O. Cherkaoui, Removal of two cationic dyes from a textile effluent by filtration–adsorption on wood sawdust, Environ. Sci. Pollut. Res. 14 (4) (2007) 237–240.

[2] G. McKay, M.S. Otterburn, D.A. Aga, Fullers earth and fired clay as adsorbent for dye stuffs, equilibrium and rate constants, Water Air Soil Pollut. 24 (3) (1985) 307–322.

[3] O. Hamdaoui, Dynamic sorption of methylene blue by cedar sawdust and crushed brick in fixed bed columns, J. Hazard. Mater. 38 (2) (2006) 293–303.

[4] B.H. Hameed, A.T.M. Din, A.L. Ahmad, Adsorption of methylene blue onto bamboo-based activated carbon: kinetics and equilibrium studies, J. Hazard. Mater. 14 (3) (2007) 819–825.

[5] B.H. Hameed, M.I. El-Khaiary, Removal of basic dye from aqueous medium using a novel agricultural waste material: pumpkin seed hull, J. Hazard. Mater. 155 (3) (2008) 601–609.

[6] V.J.P. Vilar, C.M.S. Botelho, R.A.R. Boaventura, Methylene blue adsorption by algal biomass based materials: biosorbents characterization and process behavior, J. Hazard. Mater. 147 (1–2) (2007) 120–132.

[7] E. Demirbas, M. Kobya, M.T. Sulak, Adsorption kinetics of a basic dye from aqueous solutions onto apricot stone activated carbon, Bioresour. Technol. 99 (13) (2008) 5368–5373.

[8] N. Ahalya, T.V. Ramachandra, R.D. Kanamadi, Biosorption of heavy metals, Res. J. Chem. Environ. 7 (2003) 71–78.

[9] A.A. Ahmad, B.H. Hameed, N. Aziz, Adsorption of direct dye on palm ash: kinetic and equilibrium modeling, J. Hazard. Mater. 141 (1) (2007) 70–76.

[10] A. Mittal, L. Krishnan, V.K. Gupta, Removal and recovery of malachite green from wastewater using an agricultural waste material, de-oiled soya, Sep. Purif. Technol. 43 (2) (2005) 125–133.

[11] B.H. Hameed, M.I. El-Khaiary, Sorption kinetics and isotherm studies of a cationic dye using agricultural waste: broad bean peels, J. Hazard. Mater. 154 (1–3) (2008) 639–648.

[12] B.H. Hameed, H. Hakimi, Utilization of durian (*Durio zibethinus* Murray) peel as low cost sorbent for the removal of acid dye from aqueous solutions, Biochem. Eng. J. 39 (2) (2008) 338–343.

[13] G. McKay, J.F. Porter, G.R. Prasad, The removal of basic dyes aqueous solution by adsorption on low-cost materials, Water Air Soil Pollut. 114 (3–4) (1999) 423–438.

[14] H. Serencam, A. Gundogdu, Y. Uygur, B. Kemer, V.N. Bulut, C. Duran, M. Soylak, M. Tufekci, Removal of cadmium from aqueous solution by Nordmann fir (*Abies nordmanniana* (Stev.) Spach. Subsp. *nordmanniana*) leaves, Bioresour. Technol. 99 (2008) 1992–2000.

[15] S.D. Khattri, M.K. Singh, Color removal from synthetic dye wastewater using a biosorbent, Water Air Soil Pollut. 120 (3–4) (2000) 283–294.

[16] H. Hasar, Adsorption of nickel (II) from aqueous solution onto activated carbon prepared from almond husk, J. Hazard. Mater. 97 (1–3) (2003) 49–57.

[17] M. Urrestarazu, G.A. Martinez, M.C. Salas, Almond shell waste: possible local rock wool substitute in soilless crop culture, Sci. Hortic. 103 (4) (2005) 453–460.

[18] B.N. Estevinho, E. Ribeiro, A. Alves, L. Santos, A preliminary feasibility study for pentachlorophenol column sorption by almond shell residues, Chem. Eng. J. 136 (2–3) (2008) 188–194.

[19] S. Sadhasivam, S. Savitha, K. Swaminathan, Exploitation of *Trichoderma harzianum* mycelial waste for the removal of rhodamine 6G from aqueous solution, J. Environ. Manag. 85 (1) (2007) 155–161.

[20] A. Özer, G. Dursun, Removal of methylene blue from aqueous solution by dehydrated wheat bran carbon, J. Hazard. Mater. 146 (1–2) (2007) 262–269.

[21] B. Pan, B. Pan, W. Zhang, Q. Zhang, Q. Zhang, S. Zheng, Adsorptive removal of phenol from aqueous phase by using a porous acrylic ester polymer, J. Hazard. Mater. 157 (2–3) (2008) 293–299.

[22] W.T. Tsai, H.C. Hsub, T.Y. Su, K.Y. Lin, C.M. Lin, Removal of basic dye (methylene blue) from wastewaters utilizing beer brewery waste, J. Hazard. Mater. 154 (1–3) (2008) 73–78.

[23] R. Han, W. Zou, W. Yu, S. Cheng, Y. Wang, J. Shi, Biosorption of methylene blue from aqueous solution by fallen phoenix tree's leaves, J. Hazard. Mater. 141 (1) (2007) 156–162.

[24] I. Langmuir, The adsorption of gases on plane surfaces of glass, mica and platinum, J. Am. Chem. Soc. 40 (1918) 1361–1403.

[25] K.R. Hall, L.C. Eagleton, A. Acrivos, T. Vermeulen, Pore and solid diffusion kinetics in fixed bed adsorption under constant pattern conditions, Ind. Eng. Chem. Fundam. 5 (1966) 212–223.

[26] H.M.F. Freundlich, Über die adsorption in lösungen, Ind. Eng. Chem. Fundam. 57 (1906) 385–470.

[27] S. Lagergren, About the theory of so-called adsorption of soluble substance, Kung. Sven. Veten. Hand. 24 (1898) 1–39.

[28] A.E. Ofomaja, Sorptive removal of methylene blue from aqueous solution using palm kernel fibre: effect of fibre dose, Biochem. Eng. J. 40 (1) (2008) 8–18.

[29] C. Aharoni, D.L. Sparks, Kinetics of soil chemical reactions: a theoretical treatment, in: D.L. Sparks, D.L. Su'arez (Eds.), Rates of Soil Chemical Processes, Soil Science Society of America, Madison, Wisconsin, 1991, pp. 1–18.

[30] Y.S. Ho, G. McKay, Kinetic models for the sorption of dye from aqueous solution by wood, J. Environ. Sci. Health Part B: Process Saf. Environ. Prot. 76 (4) (1998) 183–191.

[31] M. Alkan, M. Doğan, Y. Turhan, Ö. Demirbaş, P. Turan, Adsorption kinetics and mechanism of maxilon blue 5G dye on sepiolite from aqueous solutions, Chem. Eng. J. 139 (2008) 213–223.

[32] W.J. Weber Jr, J.C. Morriss, Kinetics of adsorption on carbon from solution, J. Sanitary Eng. Div. Am. Soc. Civ. Eng. 89 (1963) 31–60.

[33] S.M. Maliyekkal, S. Shukla, L. Philip, I.M. Nambi, Enhanced fluoride removal from drinking water by magnesia-amended activated alumina granules, Chem. Eng. J. 140 (2008) 183–192.

[34] E. Bulut, M. Özacar, İ.A. Şengil, Adsorption of malachite green onto bentonite: equilibrium and kinetic studies and process design, Microporous Mesoporous Mater. 115 (2008) 234–246.

[35] J.M. Smith, H.C. Van Ness, Introduction to Chemical Engineering Thermodynamics, fourth ed.McGraw-Hill, Singapore, 1987.

[36] R. Han, Y. Wang, P. Han, J. Shi, J. Yang, Y. Lu, Removal of methylene blue from aqueous solution by chaff in batch mode, J. Hazard. Mater. 137 (1) (2006) 550–557.

[37] M. Khormaei, B. Nasernejad, M. Edrisi, T. Eslamzadeh, Copper biosorption from aqueous solutions by sour orange residue, J. Hazard. Mater. 149 (2) (2007) 269–274.